J Mol Model (2010) 16:759–770
DOI 10.1007/s00894-009-0581-3

ORIGINAL PAPER

Molecular dynamics simulation of a carboxy murine neuroglobin mutated on the proximal side: heme displacement and concomitant rearrangement in loop regions

Jia Xu · Guowei Yin · Feijuan Huang · Baohuai Wang · Weihong Du

Received: 10 June 2009 / Accepted: 17 August 2009 / Published online: 8 October 2009

Abstract Neuroglobin, a member of vertebrate globin family, is distributed primarily in the brain and retina. Considerable evidence has accumulated regarding its unique ligand-binding properties, neural-specific distribution, distinct expression regulation, and possible roles in processes such as neuron protection and enzymatic metabolism. Structurally, neuroglobin enjoys unique features, such as bis-histidyl coordination to heme iron in the absence of exogenous ligand, heme orientational heterogeneity, and a heme sliding mechanism accompanying ligand binding. In the present work, molecular dynamics (MD) simulations were employed to reveal functional and structural information in three carboxyl murine neuroglobin mutants with single point mutations F106Y, F106L and F106I, respectively. The MD simulation indicates a remarkable proximal effect on detectable displacement of heme and a larger tunnel in the protein matrix. In addition, the mutation at F106 confers on the CD region a very sensitive mobility in all three model structures. The dynamic features of neuroglobin demonstrate rearrangement of the inner space and highly active loop regions in solution. These imply that the conserved residue at the G5 site plays a key role in the physiological function of this unusual protein.

Keywords Molecular dynamics simulation · Murine neuroglobin · Mutants · Proximal side

Abbreviations

Ngb	Neuroglobin
Hb	Hemoglobin
Mb	Myoglobin
MD	Molecular dynamics
CO	Carbon monoxide
F106LNgb	F106L neuroglobin mutant
NgbCO	Carboxy neuroglobin
F106YNgbCO	Carboxy neuroglobin of F106Y mutant
F106LNgbCO	Carboxy neuroglobin of F106L mutant
F106INgbCO	Carboxy neuroglobin of F106I mutant

Introduction

The vertebrate globin family comprises hemoglobin (Hb), myoglobin (Mb), neuroglobin (Ngb), cytoglobin (Cgb) [1], Globin E (Gb E) [2] and Globin X (Gb X) [3]. Neuroglobin (Ngb), a descendant of ancestral globin, was discovered in 2000 among uncharacterized expressed sequence tags (ESTs) in human and murine libraries [4]. The addition of Ngb to the globin superfamily fueled research interest in the phylogeny, regulation, and molecular evolution of this family [5, 6]. Like Hb and Mb, Ngb reversibly binds gaseous ligands like O_2, CO and NO. However, Ngb has distinct evolutionary, functional, and structural attributes

Electronic supplementary material The online version of this article (doi:10.1007/s00894-009-0581-3) contains supplementary material, which is available to authorized users.

J. Xu · G. Yin · F. Huang · W. Du (✉)
Department of Chemistry, Renmin University of China,
Beijing 100872, China
e-mail: whdu@chem.ruc.edu.cn

B. Wang
Institute of Physical Chemistry, Peking University,
Beijing 100871, China

that suggest an "uncommon role" in the physiological environment [7–15].

Based on updated evolutionary theory, the predominant role of this globin more likely resides in the enzymatic realm, like NADH oxidase in cellular surroundings [6, 16], than in the widely accepted concept of O_2 carrier [17]. The average low concentration of Ngb (~1 μM) [6] in the brain relative to Mb (~100–400 μM) [18] in the muscle impairs its ability to act as a transporter and reservoir of oxygen. In contrast, the high concentration of Ngb (100 μM) in mammalian retinal neurons [12] is seemingly indicative of a respiratory protein involved in mitochondrial oxygen metabolism [19]. However, many more intriguing features, such as intracellular signaling, the scavenging of toxic species, and NO metabolism, have been attributed to this protein [20, 21]. Ngb has been identified as a redox-coupled sensor that modulates G-protein transduction pathways [22, 23]. Overexpression of Ngb appears to have a neuroprotective role during ischemia and hypoxia in brain, and may have potential in clinical therapy [24–32].

Although a member of the same globin family, Ngb exhibits certain structural disparities compared with its relatives Hb and Mb. Ngb shares only 20–25% amino acid sequence identity with Hb and Mb [4]. However, it displays a typical globin monomeric 3-over-3 helix sandwich structure and the conserved residues that influence the heme pocket environment in this family [e.g., Phe28(B10), Phe42(CD1), Tyr44(CD3), Val68(E11), Leu92(F4), Val99 (FG3), Val101(FG5), Phe106(G5) and Val140 (H15)] [33, 34]. Nevertheless, as the first hexacoordinate vertebrate globin, Ngb displays a ligand-binding mechanism distinct from that of other pentacoordinate globins [35–38]. The crystal structures of human Ngb [33], murine Ngb [39] and carboxy murine Ngb (NgbCO) [34] have provided substantial structural insights into its functional role. The huge inner cavities, much larger than those of Mb and Hb, as well as a unique heme sliding mechanism (via reshaping of the internal tunnel), have been identified by measuring the inner cavities after CO binding [34]. NMR spectroscopy also revealed a significant equilibrium of heme orientational heterogeneity in Ngb solutions [40, 41]. Additionally, the notably ligand-induced regulation of conformation and mobility in the CD and EF loop regions indicates potential enzymatic and signal correlation.

As we know, proximal effects studies of hemoproteins are usually concentrated on the fifth ligand, His(F8) [42, 43]. In fact, some heme pocket residues on the proximal side share the same significance (Fig. 1). The Phe106(G5) residue (F106), the fifth residue of the proximal G helix in Ngb, has a fast relaxation side chain proton (T_1≈20 ms) [40] that indicates a close contact with heme. As a key site in the heme pocket, F106 locates at the gate position of the EF loop and participates in regional regulation and heme-

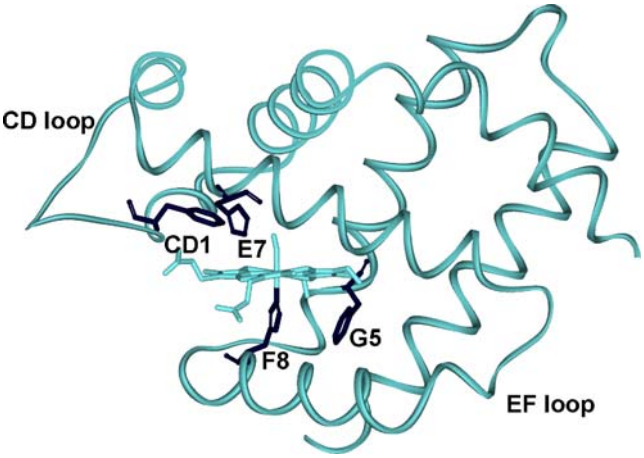

Fig. 1 Structure of carboxy murine neuroglobin (NgbCO; PDBID: 1W92). Phe42(CD1), His64(E7), His96(F8), Phe106(G5) are highlighted

residue interaction [34]. Similar behaviors have been seen in human Mb, despite the presence of leucine at the G5 site [44]. However, because the three dimensional NMR structure of Ngb is not available, the suggested role of residue G5 is basically based on position information obtained from X-ray crystallography [34, 39]. Therefore, to investigate significant features of the G5 residue in solution, and to elucidate the influence of a single point mutation of residue F106 on heme pocket properties and loop mobility, molecular dynamics (MD) simulation was chosen to create a pure system for the emulation of a single-molecular "in silico" experiment [45, 46].

MD investigations have been used to detect structural and dynamic properties of cytochrome [47, 48] and other heme-containing globins, including Hb [49, 50], and Mb [51–53]. More recently, MD has been used to simulate wild type Ngb in order to examine dynamic structural characters [54–56]. In the present work, comparative MD simulations were employed to model the structural variations in Ngb mutants at the G5 site (F106Y, F106L, F106I), and to find new dynamic and structural features. The dynamic contents during the simulation process indicate potential heme displacement and simultaneous loop regulation in these Ngb mutants and hint at corresponding functional implications.

Methods

NgbCO (PDBID:1W92) was chosen as the initial structure for characterization of the major component of two heme orientational isomers [34, 40]. The Biopolymer package, Sybyl version 7.3 (Tripos, St. Louis, MO) [57] was used to mutate Phe106 to residue Tyr, Leu, and Ile, respectively, by replacing the side chain of the residue while leaving the backbone unaltered. MD simulations with mutants

F106YNgbCO, F106LNgbCO, F106INgbCO and the control sample NgbCO were carried out using a standard parm94 force field [58] in the AMBER 9 package (Scripps, La Jolla, CA) [59]. Parameters for the heme section adopted contributions of the Amber all-atom force field from Giammona and Case [60], which maintains heme in a CO-bound state. The protein was solvated in a truncated octahedral box of water containing 6,760 TIP3P water molecules. Moderate Langevin dynamics [45, 61, 62] was adopted for the whole system with a collision frequency of $\gamma=1$ ps^{-1} to enhance the efficiency of conformational sampling in a solvated state. The nonbonded interaction cutoff value was 10.0 Å. The SHAKE algorithm, with a tolerance of 10^{-6}, was turned on to fix all bond lengths involving hydrogen atoms during the MD run [63]. The time-step was constant at 2 fs.

A total of 3,000 cycles of energy minimization were implemented to remove bad steric contacts. The first stage of the MD process was performed as reported [64], heating and equilibrating the system was then triggered. The following heating process was used: (1) MD simulation with restraining solute atomic position by harmonic potential at 10 K for 10 ps; (2) MD simulation on all atoms to equilibrate the whole system for 20 ps; (3) MD simulation with restraining solute atomic position by harmonic potential at 50 K for 10 ps. After this operation, the systematic temperature was increased for every 20 ps MD calculation (i.e., 100 K, 150 K, ... 300 K). After the heating process, the whole system was equilibrated at 300 K for 100 ps. A 60 ns production of the MD simulation was then implemented under periodical boundary conditions in an NTP ensemble at 300 K and 1 atm, using Berendsen temperature coupling [65] and isotropic molecule-based scaling. MD trajectory analysis was performed by the PTRAJ module in AMBER 9.

The conformation of model structure was analyzed using MOLMOL software [66], and the SURFNET package [67] was employed to locate interior protein cavities and to calculate their volumes. Clefts were defined with filling gap spheres upon a variable radius ($r_{min}=1.0$ Å, $r_{max}=3.0$ Å) [51, 55]. Gap volumes were calculated by erasing the CO ligand. Additionally, a cavity was judged as "exposed" if it had an interface with the solvent. All cavities were mapped by the SURFACE and SURFPLOT modules in the SURFNET package.

Results

Protein structures

Table 1 compares the different root-mean-square deviation (RMSD) between crystal structures and mean structures of MD models. An obvious reduction in RMSD values can be observed when the CD loop was excluded. Through a 60 ns MD run, the systems achieved equilibrium and the engineered structures appeared comparatively stable (see Fig. S1 in the electronic supplementary material for RMSD of the three mutants). Trajectories beyond the first 5 ns were taken as the equilibrium portion for further analysis. With a mean backbone RMSD of 1.39 Å, the model structures were acceptable and consistent with the NgbCO structure. Three model structures of Ngb mutants induced structural variability that was detected by movement of the heme relative to the protein matrix. Essential dynamics analysis was performed on all heme atoms (the terminal propionic chains were excluded) to monitor the heme motion properties in simulations. Heme motion projected onto the first eigenvector (EV1) corresponded to heme sliding [55]. The trajectories of heme displacements along EV1 reported the position of heme as a function of time (Fig. 2). The heme position distribution along EV1 (Fig. 3) is quite different between NgbCO and the three mutants. For NgbCO, the heme position mainly occupies a negative value (−2.1 Å) that corresponds to the heme position in carboxy Ngb [55]. However, the other three mutants are characterized by two maxima, while the more favorable configurations exhibit slight displacement towards positive values corresponding to the heme position in metNgb [55]. Thus, comparison of the distributions along EV1 for the four structures reveals that mutation of F106 widens the range of heme position fluctuation, mainly inducing a slightly upward heme displacement.

As mentioned above, the side chain of Phe106 in wild type Ngb has close contact with heme, and both the heme pyrrole plane and the vinyl double bond are near the aromatic Phe106. Accordingly, a possible effect induced by a single point mutation at this position might partially diminish the interaction between heme and the surrounding residues, which could potentially be a factor in the maintenance of stably docked heme.

Table 1 Comparison of root-mean-square deviation (RMSD) values between the six Ngb proteins: *upper right cells* values calculated for the whole protein; *lower left cells* values calculated excluding the CD region. All data were calculated using the VMD software package (http://www.ks.uiuc.edu/Research/vmd/)

	1W92[a]	1Q1F[a]	NgbCO	F106Y	F106L	F106I
1W92[a]	0	0.547	0.985	1.001	1.002	1.145
1Q1F[a]	0.463	0	1.064	1.037	1.132	1.210
NgbCO	0.726	0.759	0	0.641	0.659	0.849
F106Y	0.748	0.848	0.371	0	0.725	0.830
F106L	0.814	0.921	0.485	0.405	0	0.867
F106I	0.755	0.842	0.461	0.479	0.456	0

[a] Crystal structure from PDB used directly

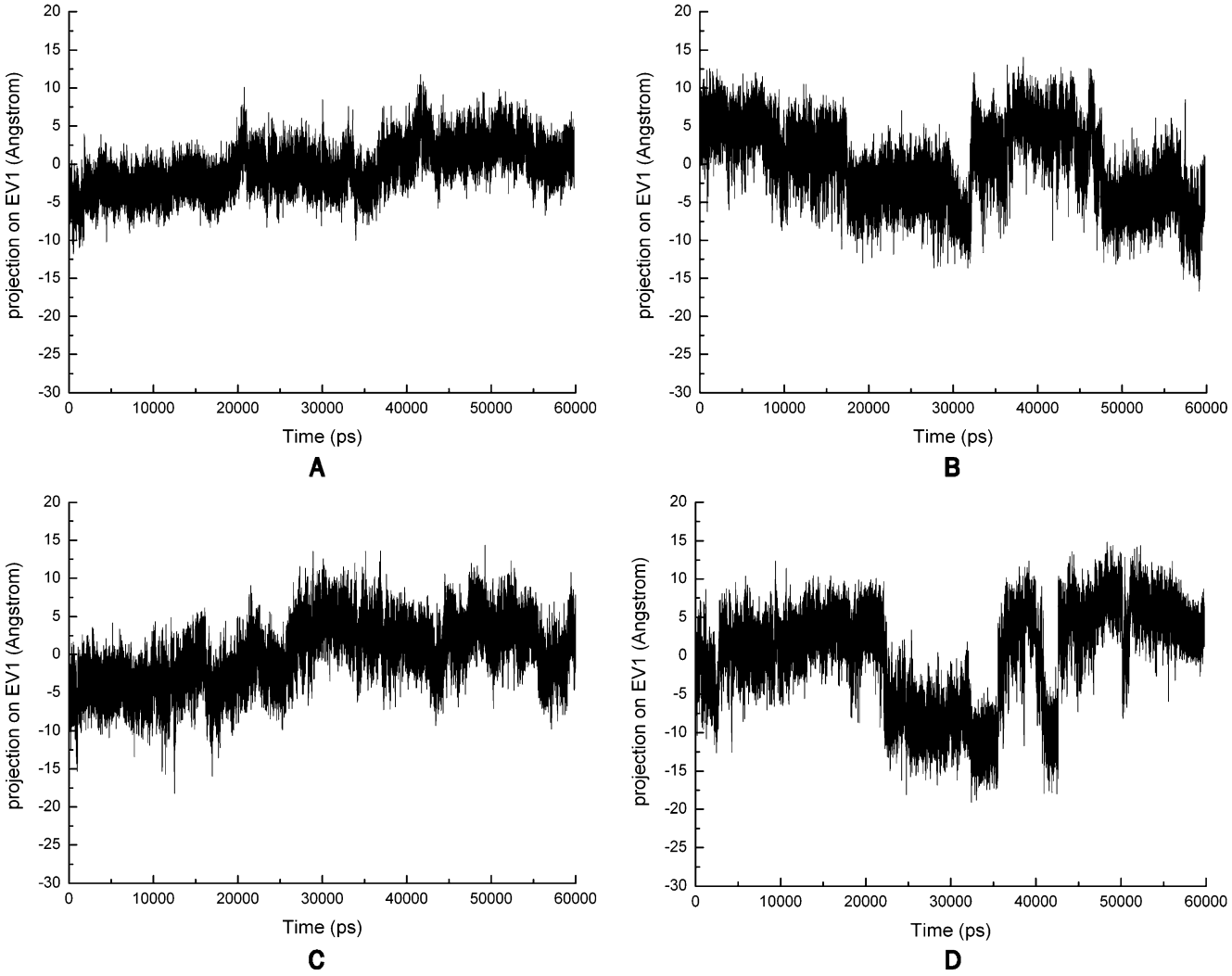

Fig. 2 Trajectories of the heme displacement along its first eigenvector (EV1) in NgbCO (**a**), and mutants F106YNgbCO (**b**), F106LNgbCO (**c**), and F106INgbCO (**d**)

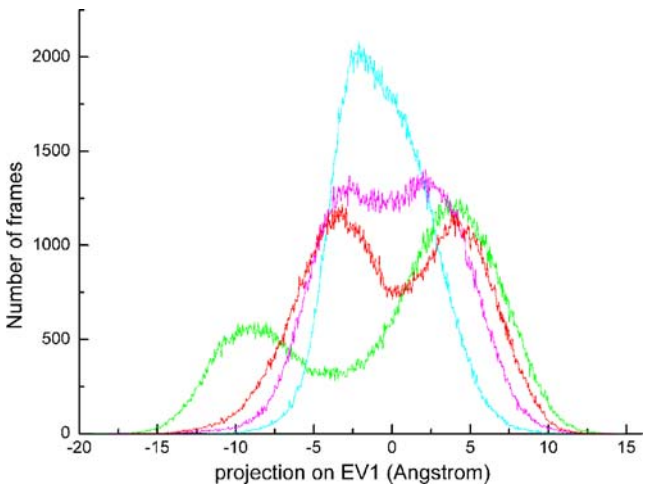

Fig. 3 Distributions of heme displacement along the EV1 in NgbCO (*cyan*), and mutants F106YNgbCO (*red*), F106LNgbCO (*purple*), and F106INgbCO (*green*)

Loop regions

B-factors based on the RMSD fit to the average structure calculated by the PTRAJ module in Amber software were used to investigate regional flexibility during dynamic simulation. The B-factors of the Cαs for all the mutants and the NgbCO control during MD simulations are shown in Fig. 4. The regional dynamic features of the four structures were consistent in solution simulation but varied partially at some specific regions. The obvious flexibilities of the EF loop in all simulated structures were similar (around Asp81 and Ser84). Moreover, there was stronger fluctuation, to some extent, than that observed by crystallography in all the loop regions in the solution environment (around Gly100, Arg102 and Pro123). In addition, with the exception of F106LNgbCO, whose relative low B-factor still reflected the influence of various mutations on loop mobility, the CD loop showed a notable increase in flexibility (around Gly46,

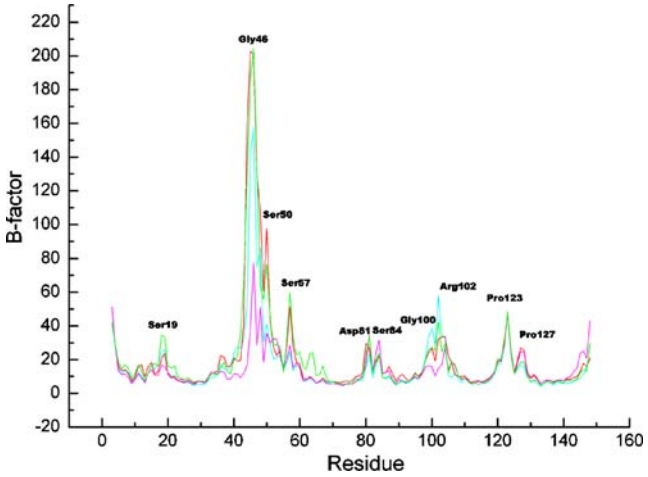

Fig. 4 B-factors (Å^2) of the average structure of mutants NgbF106YCO (*red*), NgbF106LCO (*purple*), NgbF106ICO (*green*), and the control NgbCO (*cyan*)

Ser50 and Ser57). The dynamic behavior of mutant proteins in water (via the B-factor) revealed that, in general, the inherent helix regions remained constant, but loop regions were quite active, including FG and GH corners.

Unexpectedly, the obvious enhancements of B-factor in the CD–D region after proximal mutation demonstrate that this portion is more active in Ngb structural regulation. It is possible that the CD loop is a highly active region that acts as a ligand pathway [6] and interact with the G_α subunit of the $G_{\alpha\beta\gamma}$ protein [23, 56]. More importantly, part of the CD region undergoes a topological rearrangement after MD simulation due to its close proximity to heme. This fragment, comprised of Phe42, Gln43 and Tyr44, was inclined to form tight contacts. MOLMOL analysis showed that the fragment formed a short 3^{10} helix in both F106YNgbCO and F106LNgbCO, but not in F106INgbCO during the MD run (data not shown). Considering heme movement, a larger space was found between the CD loop and heme in mutant proteins than in NgbCO. Consequently, the CD loop is subjected to regulation and facilitates the accommodation of heme motion.

Cavity properties

The inner space of NgbCO and the mutants were defined and mapped, exposing cavities that resemble those found in Mb [68] and NgbCO crystals [34]. All cavities might act as temporary docking sites for ligand binding, implying a possible physiological role [69, 70]. During the MD simulation, cavities fluctuate greatly, with volumes varying from zero to twice that of the crystal value [51, 69]. In Table 2, we report the occurrence of cavities corresponding to special sites defined as in sperm whale Mb [68] during the MD trajectories, although in Ngb different cavities tend to combine together. In order to clearly visualize cavity

Table 2 Occurrence of each cavity in the 60-ns molecular dynamics (MD) trajectories (% of time)

	DP	Xe1	Xe2	Xe3	Xe4	Ph1
NgbCO	0.70	16.58	80.01	17.99	4.23	18.17
F106Y	0.67	25.17	84.73	20.13	10.74	28.19
F106L	0.79	26.54	89.42	15.00	14.22	33.81
F106I	1.92	22.82	80.84	18.29	9.76	23.17

properties, mean structures of NgbCO and the three mutants are shown in Figure 5. It can be seen that the three mutants reveal various proximal cavities. However, cavities with lower than 5% occurrence in the trajectories could barely be observed in the mean structures. Besides isolated Ph1, Xe1, Xe4 in the three mutants, the larger tunnel that merged Xe2 and Xe4, and extended to the solvent, was surrounded by residues Gly24(B6), Leu27(B9), Phe28(B10), Phe42(CD1), His64(E7), Ile65(E8), Lys67(E10), Val68(E11), Met69 (E12), Leu70(E13), Val71(E14), Ile72(E15), Leu89(F1), Leu113(G12), Leu136(H11), Tyr137(H12) and Val140 (H15) in all four models. The average change in volume of this tunnel from 332 Å^3 in NgbCO to 359 Å^3, 354 Å^3, 411 Å^3 in F106YNgbCO, F106LNgbCO and F106INgbCO, respectively, could be ascribed to the slight displacement of heme. Although heme moves in different modes in the three mutants, the increasing tunnel volume is plausible due to the rearrangement of the loop regions.

Note that SURFNET, using parameters from Vallone et al. [39], was capable of reflecting the relative volume change of the cavity even when the tunnel volume differed from that of crystal NgbCO [34]. Under the same SURFNET conditions, a series of cavities was found between the loop and heme that provide a potential pathway of ligand entrance and escape. The cavities occupy mainly the CD and EF regions, and instantaneously link several cavities distributed at the surface and interior of the protein.

Heme pocket rearrangements

According to the superimpositions of F106Ngb mutants and NgbCO, from the reference of the porphyrin plane, the ring of His96(F8) that connects with the heme iron is tilted after simulation; the ensemble average orientation angle between His96 ring and heme (NB as x-axis) is 120.9±12.9°, 125.9± 13.7°, 114.0±13.0° and 121.0±10.8° for NgbCO, F106Y-NgbCO, F106LNgbCO, and F106INgbCO, respectively (Fig. 6, and see Fig. S2 in electronic supplementary material for trajectories of the angles).

As in some Mbs, the side chain of residue His64(E7) acts as a proton donor to the oxygen atom of bound CO, which is a significant factor in stabilizing the iron-bound ligand [71]. Simulations of the χ_1 torsion angles of His64

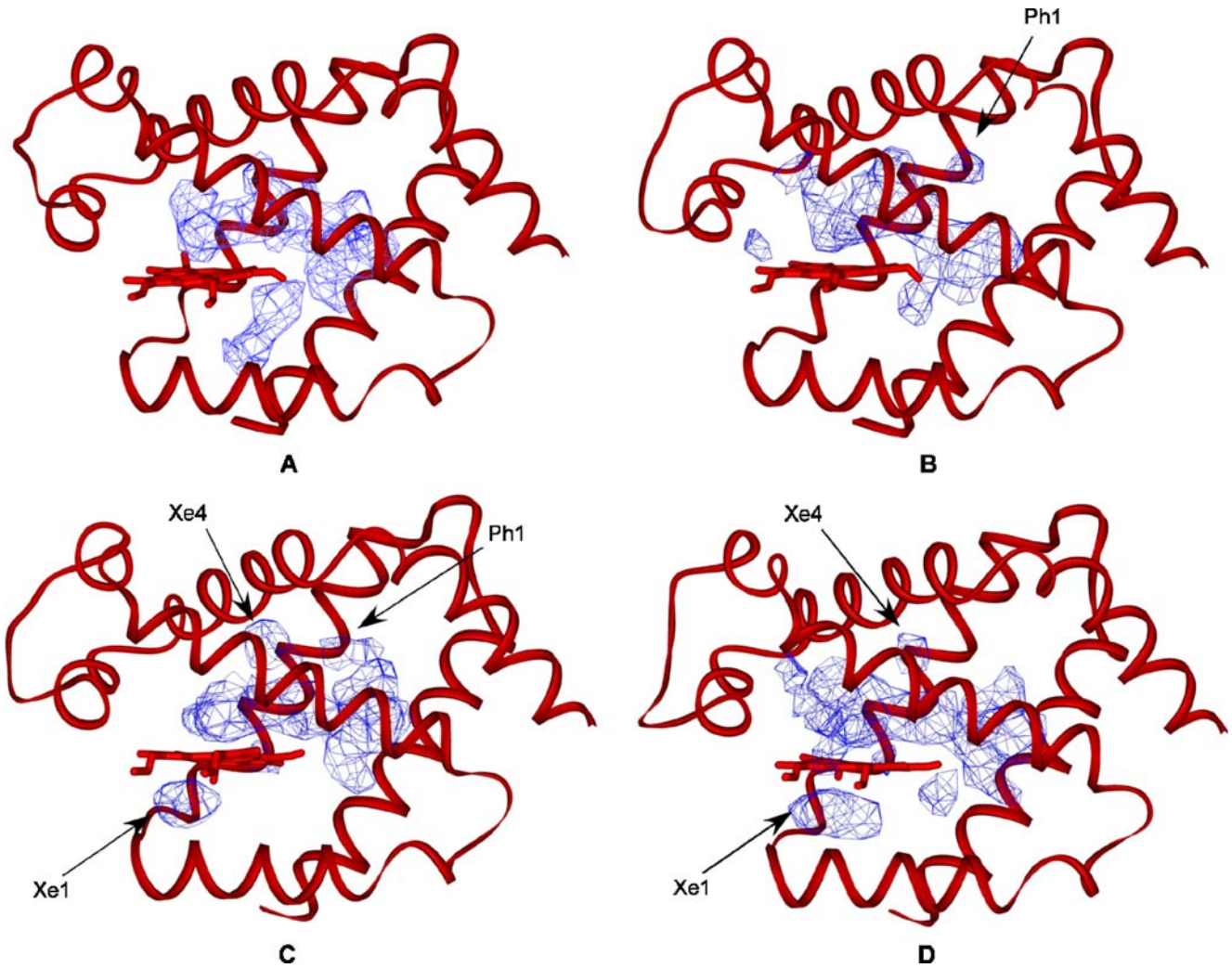

Fig. 5 Internal cavities (*blue mesh*) found by Surfnet in the mean structures of NgbCO (**a**), F106YNgbCO (**b**), F106LNgbCO (**c**) and F106INgbCO (**d**). Isolated cavities such as Xe1, Xe4, Ph1 are labeled

(E7) were carried out for the four model structures. Figure 7 shows the trajectories of E7 χ_1 angles, which are indicative of the changes of surrounding hydrophobic forces and distal cavity fluctuations. Compared with 169° in the X-ray structure (PDBID: 1W92), the E7 χ_1 angle fluctuates between 100° to 150° at the beginning of each trajectory. Within 7 ns, the E7 χ_1 angles all move up obviously except for F106LNgbCO, whose E7 χ_1 angle remains stable around 150° until 56 ns. However, a considerable shift in χ_1 angle can be observed in the F106INgbCO trajectory after 20 ns, which may suggest His-gate opening.

Discussion

Structural variability from mutation

The predominant mechanism of heme sliding depends on coordination of the exogenous ligand, which presents a significantly repositioned Phe106 (G5) at a distance of 3.8 Å in the NgbCO crystal structure [34]. As mentioned above, Phe106 is located at the hydrophobic region of the heme pocket so that heme and residue side chains interact, thereby contributing to conformational conservation of the active site around heme [72]. The aromatic residues extending into the heme pocket (e.g., Phe at B10, CD1 and G5, Tyr at CD3 and H12), could maintain the hydrophobic environment with each other or with heme. MD simulations of the distinct G5 site mutation of Ngb expose potential structural variability and allude to proximal effects on heme sliding and regional modulation.

The simulation structures have a visibly upward or tilted position for heme transfer, which could be affected by the mutation. Due to the G5 site mutation in Ngb, the interaction network in heme-adjacent space is subjected to topological readjustment via bond torsion and displacement of residue side chains so as to obtain an energy- optimized structure. Accordingly, slight movements of heme cannot

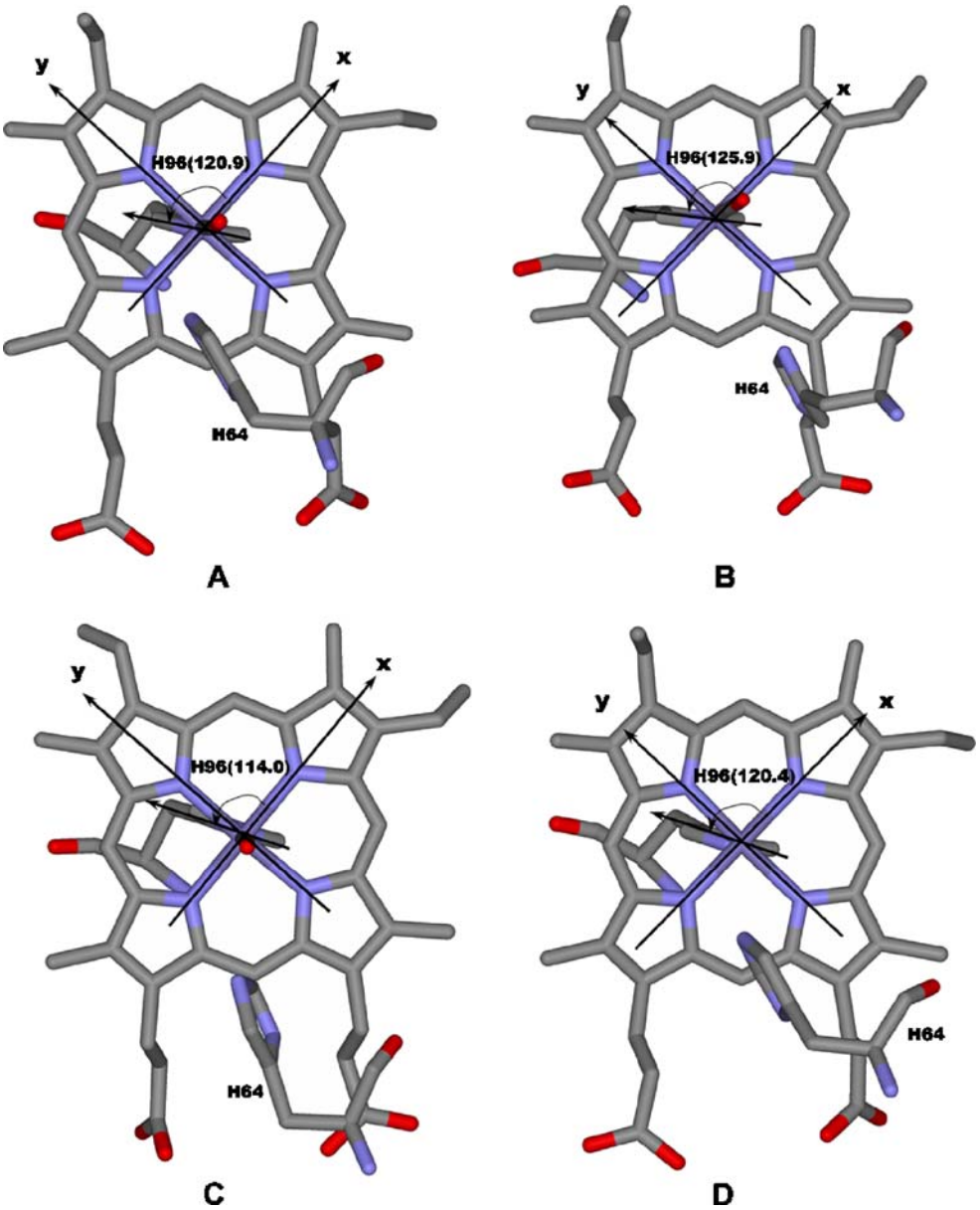

Fig. 6 Average orientation angles between the His96(F8) ring plane and heme in NgbCO (**a**), F106YNgbCO (**b**), F106LNgbCO(**c**), and F106INgbCO (**d**)

be ignored. Such transfer of heme position with respect to a relatively invariable protein matrix could impact the entrance of exterior gas molecules in two ways: through the residue interaction network, and via accessible inner spaces. Spatial comparisons of individual mutant structures obtained from MD reveal variation in the orientation and position of each residue that might play a key role in heme cavity properties. As the fifth axial ligand, the tilt of the aromatic ring of His96 corresponds to a change in molecular energy and configuration about the iron-centered octahedron ligand field, which supposedly weakens the bond strength between exogenous ligand and iron, and leads to the sixth ligand adopting an unfavorable orientation in the distal pocket.

Large internal cavities are distinct structural features of Ngb. The rearrangement of heme occurs in all three mutants along the remarkable tunnel that covers most of the distal heme pocket and provides a link to the outer space. Such a vast cleft in Ngb possibly facilitates heme orientation and ligand tilt by reshaping the heme pocket and providing more potential pathways that open instantaneously. As a consequence of Ngb structural regulation, measured tunnel volumes are larger after mutation. Heme, following the tunnel of the mutant molecule, is most likely influenced by the surrounding environment. And the tunnel provides a more spacious pathway and shorter trip for ligand release with fewer energy requirements.

Dynamic loop regions

The mutant proteins show better agreement with NgbCO regarding the flexibilities of helices A to H during the

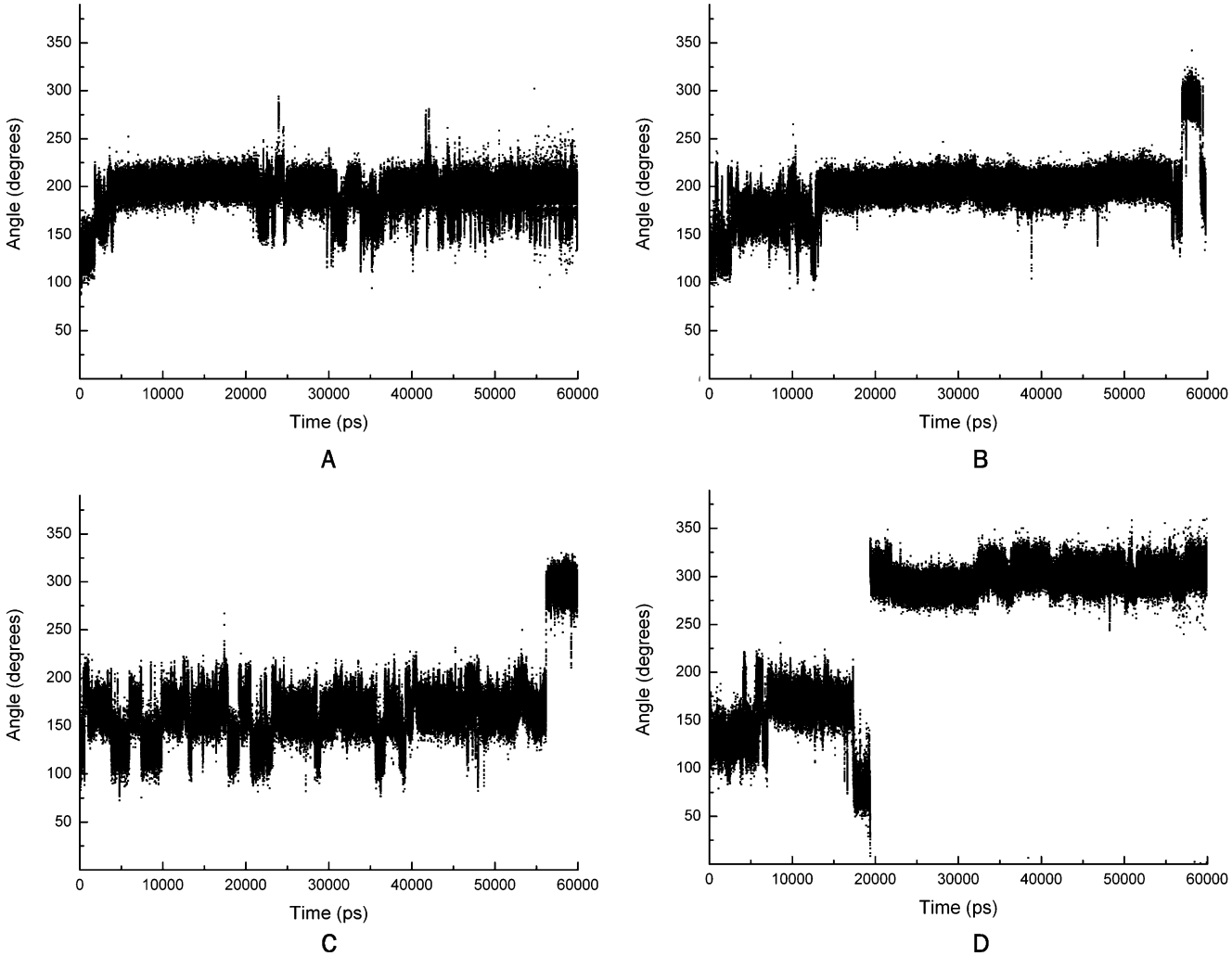

Fig. 7 Comparison of Ki angle of residue His64(E7) in NgbCO (**a**), F106YNgbCO (**b**), F106LNgbCO(**c**), and F106INgbCO (**d**)

simulation in solution. However, globin loop regions are usually highly flexible and closely connected to protein function under physiological conditions.

The Ngb mutants show a more striking fluctuation in the CD–D region than NgbCO. The central portion of the CD region with variable B-factor values (Fig. 4) is illustrative of active loop dynamics. Loop mobility might be associated with E7 χ1 angles. The lower B-factor of the CD loop in F106LNgbCO is possibly due to the relatively stable E7 χ1 angle (see Fig. 7c). Formation of the short 3^{10} helix in the fragment reveals a higher flexibility about the loop region in a solution environment than in the restricted crystal state [73]. The solvated state better resembles organismal conditions, and the CD loop is more flexible than other regions in solution since it possesses predominantly a number of unstructured residues.

The short D helix is also highly flexible, especially around residue Ser57 (B-factor: 51, 28, 60 $Å^2$ in three mutants). The flexibility of the D helix reflects another active part of protein—it rearranges when an exogenous ligand enters. The flexibility of certain protein regions characterizes a typical allosteric effect in Ngb that adjusts protein conformation to adapt to CO ligation. Recent research has found that steric regulation of the flexible CD loop and D helix has a certain significance for protein structure and function. Compared with Mb, the CD–D region is very compact. Such a compact region could function as a hinge allowing E helix displacement upon CO ligation. The high mobility of this region makes sense when considering the functional role of enzymes and intracellular signal transduction, which is possibly sensitive to ligand recognition [6].

The B-factors of Ngb mutants reveal more active regions. Besides residues 46, 57 and 81 near CD and EF regions, the sharp peaks around residue 100, 102 and 123 indicate obvious flexibility of the FG and GH loops in the mutant model structures. These results indicate that not only proximal His96 but also FG and GH corners take part

in heme rearrangement and regional modulation. The variable mobility of the FG and GH loop as well as rearrangement of the CD–D region seemingly enhances the capture and release of small molecules through the large tunnel in Ngb by the corresponding reshaping of this cavity. Moreover, such remarkable features indicate multiple docking sites and ligand pathways. Topological regulation would generate a low oxygen signal under physiological conditions, and subsequently shape interactions between Ngb and its receptor during neural protection.

Dynamic features in distal pocket

In the presence of a cooperative structural modification, residues that inhabit the distal pocket and that are highly conserved in the globin family, undergo a suitable displacement, such as the side chain movement of Phe42(CD1) (Fig. 8). Furthermore, a clearly detectable motion of the His64(E7) side chain might have a large impact on CO ligation. Formation of a hydrogen bond between the $N_{\varepsilon}H$ of His64 and the oxygen atom of CO is fundamental to the stable coordination of CO. The probability of forming this hydrogen bond decreases with the side chain of His64 swing between two states during the whole simulation (Fig. 7), leading to a larger separation between the imidazole ring and the end of CO, which is comparable to the so-called open state.

An equilibrated interacting system comprised of heme and its adjacent residues would have a large influence on the exogenous ligand entrance. The mutant might perturb the interactive system on the proximal side of the heme pocket, after which a cooperative effect would occur on the distal side through the interaction with heme via heme displacement. Topological regulation on both the proximal and distal sides could constitute a new interactive network that induces reorganization of the internal space of the protein. Following this spatial regulation, the newly positioned distal residues and cavities in Ngb would have

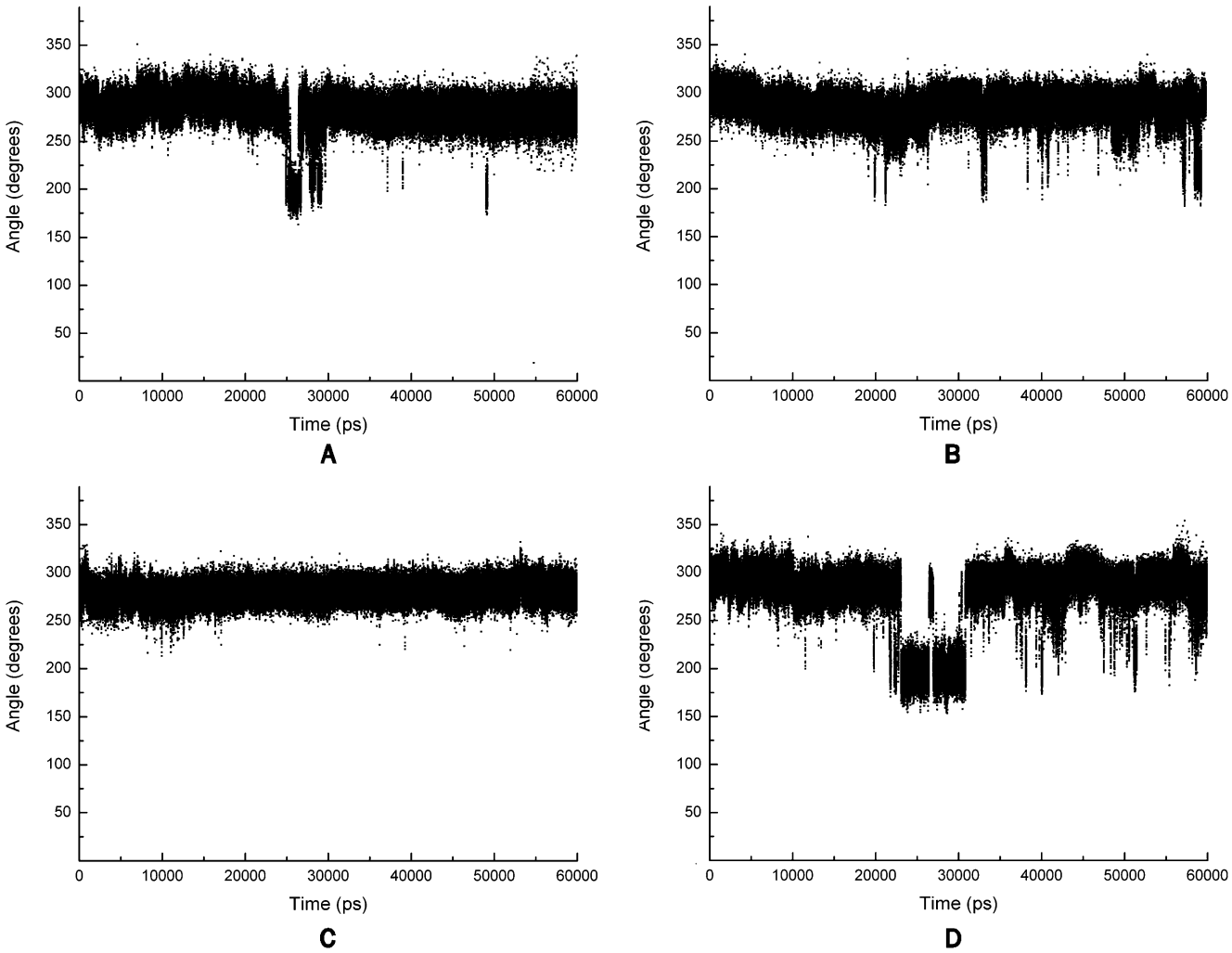

Fig. 8 Comparison of Ki angle of residue Phe42(CD1) in NgbCO (**a**), F106YNgbCO (**b**), F106LNgbCO(**c**), and F106INgbCO (**d**)

a large influence on CO ligation. The redistributed interior of Ngb could offer new pathways and docking sites for ligands, which might modestly facilitate or block the access of ligand between the outer and inner regions of the protein. An interactive network of residues in the heme pocket and the arrangement of the inner cavities could directly influence the entrance and escape of exterior molecules.

The MD simulations of the CO complex of Ngb mutants show that single point mutations at the key proximal residue F106 induce further displacement of heme and reveal the remarkable dynamic content of loop regions. The significance of the G5 site is consistent with previous results from experiments on Mb and Ngb [34, 47, 74]. A putative effect of mutation at the G5 site is the altered interaction between heme and the G5 side chain, as well as other key residues in the heme pocket. The large tunnel located in the protein matrix of Ngb is associated with facilitating exogenous ligand motion and accommodating ligands in the heme pocket. Modest changes in volume of inner cavities and acceptable loop region conformational regulation could accompany the allosteric modification of heme displacement. Furthermore, the increasing flexibility of the CD, FG, and GH regions predicts potential physiological roles of Ngb in enzymatic catalysis, signal transduction, and neuron protection in the brain.

Acknowledgments We thank Prof. Roman Laskowski at European Bioinformatics Institute (Cambridge, UK) for providing the Surfnet software and for helpful discussion. This work was supported by grants from the National Natural Science Foundation of China No. 20473013 and No. 20633080, as well as the National Basic Research Program of China (No. 2004CB719900).

References

1. Trent JT, Hargrove MS (2002) A ubiquitously expressed human hexacoordinate hemoglobin. J Biol Chem 277(22):19538–19545
2. Kugelstadt D, Haberkamp M, Hankeln T, Burmester T (2004) Neuroglobin, cytoglobin, and a novel, eye-specific globin from chicken. Biochem Biophys Res Commun 325(3):719–725
3. Roesner A, Fuchs C, Hankeln T, Burmester T (2005) A globin gene of ancient evolutionary origin in lower vertebrates: evidence for two distinct globin families in animals. Mol Biol Evol 22 (1):12–20
4. Burmester T, Weich B, Reinhardt S, Hankein T (2000) A vertebrate globin expressed in the brain. Nature 407(6803):520–523
5. Pesce A, Bolognesi M, Bocedi A, Ascenzi P, Dewilde S, Moens L, Hankeln T, Burmester T (2002) Neuroglobin and cytoglobin—fresh blood for the vertebrate globin family. EMBO Rep 3 (12):1146–1151
6. Brunori M, Vallone B (2007) Neuroglobin, seven years after. Cell Mol Life Sci 64(10):1259–1268
7. Brunori M, Vallone B (2006) A globin for the brain. FASEB J 20 (13):2192–2197
8. Fuchs C, Burmester T, Hankeln T (2006) The amphibian globin gene repertoire as revealed by the Xenopus genome. Cytogenet Genome Res 112(3–4):296–306
9. Geuens E, Brouns I, Flamez D, Dewilde S, Timmermans J-P, Moens L (2003) A globin in the nucleus! J Biol Chem 278 (33):30417–30420
10. Hankeln T, Ebner B, Fuchs C, Gerlach F, Haberkamp M, Laufs TL, Roesner A, Schmidt M, Weich B, Wystub S, Saaler-Reinhardt S, Reuss S, Bolognesi M, De Sanctis D, Marden MC, Kiger L, Moens L, Dewilde S, Nevo E, Avivi A, Weber RE, Fago A, Burmester T (2005) Neuroglobin and cytoglobin in search of their role in the vertebrate globin family. J Inorg Biochem 99(1):110–119
11. Laufs TL, Wystub S, Reuss S, Burmester T, Saaler-Reinhardt S, Hankeln T (2004) Neuron-specific expression of neuroglobin in mammals. Neurosci Lett 362(2):83–86
12. Schmidt M, Giessl A, Laufs T, Hankeln T, Wolfrum U, Burmester T (2003) How does the eye breathe? Evidence for neuroglobin-mediated oxygen supply in the mammalian retina. J Biol Chem 278(3):1932–1935
13. Sun Y, Jin K, Mao XO, Zhu Y, Greenberg DA (2001) Neuroglobin is up-regulated by and protects neurons from hypoxic-ischemic injury. Proc Natl Acad Sci USA 98(26):15306–15311
14. Sun Y, Jin K, Peel A, Mao XO, Xie L, Greenberg DA (2003) Neuroglobin protects the brain from experimental stroke invivo. Proc Natl Acad Sci USA 100(6):3497–3500
15. Wolfrum U, Giessl A, Schmidt M, Laufs T, Hankeln T, Burmester T (2003) How does the eye breathe? Evidence for neuroglobin-mediated oxygen supply in the mammalian retina. Invest Ophthalmol Vis Sci 44(5):3266
16. Brunori M, Giuffre A, Nienhaus K, Nienhaus GU, Scandurra FM, Vallone B (2005) Neuroglobin, nitric oxide, and oxygen: functional pathways and conformational changes. Proc Natl Acad Sci USA 102(24):8483–8488
17. Vinogradov SN, Hoogewijs D, Bailly X, Arredondo-Peter R, Guertin M, Gough J, Dewilde S, Moens L, Vanfleteren JR (2005) Three globin lineages belonging to two structural classes in genomes from the three kingdoms of life. Proc Natl Acad Sci USA 102(32):11385–11389
18. Wittenberg BA, Wittenberg JB (1989) Transport of oxygen in muscle. Annu Rev Physiol 51(1):857–878
19. Ostojic J, Sakaguchi DS, de Lathouder Y, Hargrove MS, Trent JT, Kwon YH, Kardon RH, Kuehn MH, Betts DM, Grozdanic S (2006) Neuroglobin and cytoglobin: oxygen-binding proteins in retinal neurons. Invest Ophthalmol Visual Sci 47(3):1016–1023
20. Burmester T, Hankeln T (2004) Neuroglobin: a respiratory protein of the nervous system. News Physiol Sci 19:110–113
21. Fordel E, Thijs L, Moens L, Dewilde S (2007) Neuroglobin and cytoglobin expression in mice—evidence for a correlation with reactive oxygen species scavenging. FEBS J 274(5):1312–1317
22. Wakasugi K, Nakano T, Morishima I (2003) Oxidized human neuroglobin acts as a heterotrimeric G alpha protein guanine nucleotide dissociation inhibitor. J Biol Chem 278(38):36505–36512
23. Kitatsuji C, Kurogochi M, Nishimura S, Ishimori K, Wakasugi K (2007) Molecular basis of guanine nucleotide dissociation inhibitor activity of human neuroglobin by chemical cross-linking and mass spectrometry. J Mol Biol 368(1):150–160
24. Nayak GH, Milton SL, Prentice HM (2007) Neuroglobin is upregulated by hypoxia and anoxia in the brain of the anoxia-tolerant turtle *Trachemys scripta*. FASEB J 21(6):A924–A924
25. Yu Z, Fan X, Lo EH, Wang X (2009) Neuroprotective roles and mechanisms of neuroglobin. Neurol Res 31(2):122–127
26. Burmester T, Hankeln T (2009) What is the function of neuroglobin? J Exp Biol 212(10):1423–1428
27. Zhou GY, Zhou SN, Lou ZY, Zhu CS, Zheng XP, Hu XQ (2008) Translocation and neuroprotective properties of transactivator-of-transcription protein-transduction domain-neuroglobin fusion protein in primary cultured cortical neurons. Biotechnol Appl Biochem 49:25–33

28. Liu J, Yu Z, Guo S, Lee SR, Xing C, Zhang C, Gao Y, Nicholls DG, Lo EH, Wang X (2009) Effects of neuroglobin overexpression on mitochondrial function and oxidative stress following hypoxia/reoxygenation in cultured neurons. J Neurosci Res 87 (1):164–170
29. Yu Z, Liu J, Guo S, Xing C, Zhu H, Yuan JC, Lo EH, Wang X (2008) Neuroglobin-overexpression alters hypoxic response gene expression in primary neuron culture following oxygen glucose deprivation. Stroke 39(2):676–676
30. Wang XY, Liu JX, Zhu HH, Tejima E, Tsuji K, Murata Y, Atochin DN, Huang PL, Zhang CG, Lo EH (2008) Effects of neuroglobin overexpression on acute brain injury and long-term outcomes after focal cerebral ischemia. Stroke 39(6):1869–1874
31. Duong TT, Witting PK, Antao ST, Parry SN, Kennerson M, Lai B, Vogt S, Lay PA, Harris HH (2009) Multiple protective activities of neuroglobin in cultured neuronal cells exposed to hypoxia reoxygenation injury. J Neurochem 108(5):1143–1154
32. Yu Z, Liu J, Guo S, Xing C, Fan X, Ning M, Yuan JC, Lo EH, Wang X (2009) Neuroglobin-overexpression alters hypoxic response gene expression in primary neuron culture following oxygen glucose deprivation. Neuroscience 162(2):396–403
33. Pesce A, Dewilde S, Nardini M, Moens L, Ascenzi P, Hankeln T, Burmester T, Bolognesi M (2003) Human brain neuroglobin structure reveals a distinct mode of controlling oxygen affinity. Structure 11(9):1087–1095
34. Vallone B, Nienhaus K, Matthes A, Brunori M, Nienhaus GU (2004) The structure of carbonmonoxy neuroglobin reveals a heme-sliding mechanism for control of ligand affinity. Proc Natl Acad Sci USA 101(50):17351–17356
35. Dewilde S, Kiger L, Burmester T, Hankeln T, Baudin-Creuza V, Aerts T, Marden MC, Caubergs R, Moens L (2001) Biochemical characterization and ligand-binding properties of neuroglobin, a novel member of the globin family. J Biol Chem 276(42):38949–38955
36. Hamdane D, Kiger L, Dewilde S, Green BN, Pesce A, Uzan J, Burmester T, Hankeln T, Bolognesi M, Moens L, Marden MC (2003) The redox state of the cell regulates the ligand binding affinity of human neuroglobin and cytoglobin. J Biol Chem 278 (51):51713–51721
37. Smagghe BJ, Sarath G, Ross E, Hilbert JL, Hargrove MS (2006) Slow ligand binding kinetics dominate ferrous hexacoordinate hemoglobin reactivities and reveal differences between plants and other species. Biochemistry 45(2):561–570
38. Trent JT, Watts RA, Hargrove MS (2001) Human neuroglobin, a hexacoordinate hemoglobin that reversibly binds oxygen. J Biol Chem 276(32):30106–30110
39. Vallone B, Nienhaus K, Brunori M, Nienhaus GU (2004) The structure of murine neuroglobin: novel pathways for ligand migration and binding. Proteins Struct Funct Bioinformat 56(1):85–92
40. Du WH, Syvitski R, Dewilde S, Moens L, La Mar GN (2003) Solution ^{1}H NMR characterization of equilibrium heme orientational disorder with functional consequences in mouse neuroglobin. J Am Chem Soc 125(27):8080–8081
41. Du WH, Yin GW, Li YJ, Wei Q, Li J, Fang WH (2007) Ligand binding affinity of cyanide complex of single mutant F106L murine-met-neuroglobin. Chem J Chin U 28(8):1547–1551
42. Capece L, Marti MA, Crespo A, Doctorovich F, Estrin DA (2006) Heme protein oxygen affinity regulation exerted by proximal effects. J Am Chem Soc 128(38):12455–12461
43. Franzen S, Peterson ES, Brown D, Friedman JM, Thomas MR, Boxer SG (2002) Proximal ligand motions in H93G myoglobin. Eur J Biochem 269(19):4879–4886
44. Liong EC, Dou Y, Scott EE, Olson JS, Phillips GN Jr (2001) Waterproofing the heme pocket. role of proximal amino acid side chains in preventing hemin loss from myoglobin. J Biol Chem 276(12):9093–9100
45. Adcock SA, McCammon JA (2006) Molecular dynamics: survey of methods for simulating the activity of proteins. Chem Rev 106 (5):1589–1615
46. Sotomayor M, Schulten K (2007) Single-molecule experiments in vitro and in silico. Science 316(5828):1144–1148
47. Bret C, Roth M, Norager S, Hatchikian EC, Field MJ (2002) Molecular dynamics study of desulfovibrio africanus cytochrome c3 in oxidized and reduced forms. Biophys J 83(6):3049–3065
48. Park H, Lee S, Suh J (2005) Structural and dynamical basis of broad substrate specificity, catalytic mechanism, and inhibition of cytochrome P450 3A4. J Am Chem Soc 127(39):13634–13642
49. Ceccarelli M, Ruggerone P, Anedda R, Fais A, Era B, Sollaino MC, Corda M, Casu M (2006) Structure–function relationship in a variant hemoglobin: a combined computational-experimental approach. Biophys J 91(9):3529–3541
50. Henry ER, Levitt M, Eaton WA (1985) Molecular dynamics simulation of photodissociation of carbon monoxide from hemoglobin. Proc Natl Acad Sci USA 82(7):2034–2038
51. Bossa C, Amadei A, Daidone I, Anselmi M, Vallone B, Brunori M, Di Nola A (2005) Molecular dynamics simulation of sperm whale myoglobin: effects of mutations and trapped CO on the structure and dynamics of cavities. Biophys J 89(1):465–474
52. Elber R, Karplus M (1987) Multiple conformational states of proteins: a molecular dynamics analysis of myoglobin. Science 235(4786):318–321
53. Hummer G, Schotte F, Anfinrud PA (2004) Unveiling functional protein motions with picosecond X-ray crystallography and molecular dynamics simulations. Proc Natl Acad Sci USA 101 (43):15330–15334
54. Nadra AD, Marti MA, Pesce A, Bolognesi M, Estrin DA (2008) Exploring the molecular basis of heme coordination in human neuroglobin. Proteins 71(2):695–705
55. Anselmi M, Brunori M, Vallone B, Di Nola A (2007) Molecular dynamics simulation of deoxy and carboxy murine neuroglobin in water. Biophys J 93(2):434–441
56. Anselmi M, Brunori M, Vallone B, Di Nola A (2008) Molecular dynamics simulation of the neuroglobin crystal: comparison with the simulation in solution. Biophys J 95(9):4157–4162
57. Tripos, International. SYBYL 7.3. St. Louis, MO
58. Cornell WD, Cieplak P, Bayly CI, Gould IR, Merz KM, Ferguson DM, Spellmeyer DC, Fox T, Caldwell JW, Kollman PA (1996) A second generation force field for the simulation of proteins, nucleic acids, and organic molecules. J Am Chem Soc 118 (9):2309–2309
59. TAD CDA, Cheatham TE III, Simmerling CL, Wang J, Duke RE, Luo R, Merz KM, Pearlman DA, Crowley M, Walker RC, Zhang W, Wang B, Hayik S, Roitberg A, Seabra G, Wong KF, Paesani F, Wu X, Brozell S, Tsui V, Gohlke H, Yang L, Tan C, Mongan J, Hornak V, Cui G, Beroza P, Mathews DH, Schafmeister C, Ross WS, Kollman PA (2006) AMBER 9. University of California, San Francisco
60. Giammona DA (1984) An examination of conformational flexibility in porphyrins and bulky-ligand binding in myoglobin. University of California, Davis, CA
61. Wu XW, Brooks BR (2003) Self-guided Langevin dynamics simulation method. Chem Phys Lett 381(3–4):512–518
62. Nutt DR, Meuwly M (2004) CO migration in native and mutant myoglobin: atomistic simulations for the understanding of protein function. Proc Natl Acad Sci USA 101(16):5998–6002
63. Ryckaert JP, Ciccotti G, Berendsen HJC (1977) Numerical integration of the cartesian equations of motion of a system with constraints: molecular dynamics of n-alkanes. J Comput Phys 23 (3):327–341
64. Hata M, Hirano Y, Hoshino T, Tsuda M (2001) Monooxygenation mechanism by cytochrome P-450. J Am Chem Soc 123(26):6410–6416

65. Berendsen HJC, Postma JPM, van Gunsteren WF, DiNola A, Haak JR (1984) Molecular dynamics with coupling to an external bath. J Chem Phys 81(8):3684–3690
66. Koradi R, Billeter M, Wuthrich K (1996) MOLMOL: a program for display and analysis of macromolecular structures. J Mol Graphics 14(1):51–55 29–32
67. Laskowski RA (1995) Surfnet—a program for visualizing molecular-surfaces, cavities, and intermolecular interactions. J Mol Graphics 13(5):323–330 307–328
68. Tilton RF, Kuntz ID, Petsko GA (1984) Cavities in proteins: structure of a metmyoglobin xenon complex solved to 1.9 Å. Biochemistry 23(13):2849–2857
69. Bossa C, Anselmi M, Roccatano D, Amadei A, Vallone B, Brunori M, Di Nola A (2004) Extended molecular dynamics simulation of the carbon monoxide migration in sperm whale myoglobin. Biophys J 86(6):3855–3862
70. Orlowski S, Nowak W (2007) Locally enhanced sampling molecular dynamics study of the dioxygen transport in human cytoglobin. J Mol Model 13(6–7):715–723
71. Springer BA, Sligar SG, Olson JS, Phillips GN (1994) Mechanisms of ligand recognition in myoglobin. Chem Rev 94(3):699–714
72. Shelnutt JA, Rousseau DL, Friedman JM, Simon SR (1979) Protein–heme interaction in hemoglobin: evidence from Raman difference spectroscopy. Proc Natl Acad Sci USA 76(9):4409–4413
73. Guallar V, Jarzecki AA, Friesner RA, Spiro TG (2006) Modeling of ligation-induced helix/loop displacements in myoglobin: toward an understanding of hemoglobin allostery. J Am Chem Soc 128(16):5427–5435
74. Draghi F, Miele AE, Travaglini-Allocatelli C, Vallone B, Brunori M, Gibson QH, Olson JS (2002) Controlling ligand binding in myoglobin by mutagenesis. J Biol Chem 277(9):7509–7519